Chapter 9

Molybdenum Disulfide-Based Photocatalysis:Bulk-to-Single Layer Structure and Related Photomechansim for Environmental Applications

Surya Veerendra Prabhakar Vattikuti and
Chan Byon

Additional information is available at the end of the chapter

http://dx.doi.org/10.5772/67825

Abstract

Bulk-to-single layer molybdenum disulfide (MoS_2) is widely used as a robust candidate for photodegradation of organic pollutants, hydrogen production, and CO_2 reduction. This material features active edge sites and narrow band gap features, which are useful for generating reactive species in aqueous suspensions. However, the high-charge carrier recombination, photocorrosion, unstable sulfide state, and formation of Mo-S-O links during photocatalytic reactions limit its applicability. Thus, research has focused on improving the performance of MoS_2 by tailoring its bulk-to-single layer structure and combining it with other semiconductor materials to improve the photocatalytic performance. Different strategies have been successfully applied to enhance the photocatalytic activity of MoS_2, including tailoring of the surface morphology, formation of heterojunctions with other semiconductors, doping, and modification with excess sulfur or carbon nanostructures. This review describes the influence of starting precursors, sulfur sources, and synthetic methods to obtain heterostructured morphologies and study their impact on the photocatalytic efficiency. Finally, the relevance of crystal facets and defects in photocatalysis is outlined. Future applications of MoS_2 with tailoring and tuning physicochemical properties are highlighted.

Keywords: layered materials, molybdenum disulfide, photocatalyst, pollutants, nanomaterials

1. Introduction

The environment continues to become more polluted due to industrialization. However, traditional chemical methods that deal with environmental pollution have been unable to meet the requirements of saving energy and environmental protection. Environmental problems

induced by toxic and organic pollutants that are hard to degrade (such as halides, dioxins, pesticides, and dyes) are important issues for human well-being and development. The sun is an abundant source of energy and sustains life on earth; and photocatalysis has been studied extensively for waste water recycling in various industries to remove organic pollutants using photocatalysts. The use of photocatalysts for waste water treatment is promising for meeting increasing water recycling demands without compromising the quality of our environment.

Although photocatalysis is successful in laboratory studies, there are some technological problems that hamper the extensive commercial applicability of this technique. Optimum utilization and commercial viability of photocatalysis could possibly be achieved by replacing the expensive and technically complex artificial light sources with low cost and renewable energy from sunlight as a natural excitation source. In recent decades, photocatalysts with high activities based on transition metal dichalcogenides (TMDs) have been used extensively for environmental applications such as air purification, water disinfection, hazardous waste remediation, and water purification. TMDs materials such as MQ_2 (M = Mo, Nb, Re, V, W and Q = S, Se) have gained much attention due to their unique properties for a wide range of applications, since the nanoscale form of these inorganic materials was discovered.

Tenne et al. [1] discovered spherical fullerene-like nanoparticles of molybdenum disulfide (MoS_2) and tungsten disulphide (WS_2) nanotubes in 1992. Since then, research on these materials and their tribological properties has intensified. One-dimensional (1D) or two-dimensional (2D) structures of TMDs materials have remarkable properties, such as chemical inertness, anisotropy, photocorrosion resistance, electronic properties, tribological properties, and photocatalytic behavior [2–8]. They also have good catalytic properties and resistance to sulfur poisoning [9]. MoS_2 and WS_2 are the most prominent family of TMDs materials and are most commonly used in layered structured forms. They have a layered, close-packed hexagonal crystal structure confined in vertically stacked monolayers that bond together by weak van der Waals forces. However, the structural and morphological features of these materials widely depend on the synthesis strategies. The starting materials, surfactants, sulfur sources, and solvents play crucial roles in the structural and morphological features.

The different morphologies of MoS_2 and WS_2 include nanospheres, few-layered nanosheets, nanofibers, nanotubes, and nanorods. These forms have attracted extensive interest owing to their intriguing physical properties and prospects for applications in nanoelectronics, electrochemistry, catalysis, and lubrication. However, the performance characteristic of these materials depends on the particle size, shape, and structure. These materials are synthesized by various approaches, including chemical vapor deposition, photothermal, sonochemical, solvothermal, hydrothermal, and two-step electrochemical synthesis methods.

2. Synthetic methods

2.1. Synthesis of MoS_2 nanomaterials

In the reaction stage, the size and shape control during the synthesis of MoS_2 nanomaterials are crucial for obtaining well-defined materials with specific properties. The morphology and

http://dx.doi.org/10.5772/67825

size of MoS_2 play a significant role in catalysis, sensors, and other applications. Shape control is also important for applications in photochemistry and fuel cell catalysis. Other factors include monodispersity, avoiding agglomeration, and surface functionalization.

The wide variety of synthetic methods for obtaining MoS_2 nanomaterials can be divided into three main groups: (i) mechanical methods (e.g., grinding, ultrasonic cracking, or milling), (ii) liquid phase methods (e.g., sol-gel, hydrothermal, or wet chemical methods), and (iii) gas phase techniques (e.g., chemical vapor deposition or laser ablation deposition). Liquid phase techniques are used most often due to their simplicity, low cost, and the wide variety of different sizes, shapes, and surface functionalities that can be obtained. Also, the size and agglomeration are effectively controlled by functionalization of the nanomaterial surface with surfactants. In some cases, these surfactants are used to control the shape and to promote growth in a specific direction by selective binding to some crystalline faces. **Figure 1** shows the SEM and TEM images of MoS_2 nanosheets synthesized by solvothermal approach [6]. These MoS_2 nanosheets were obtained as a few lamellar layers using thiourea as a sulfur source.

The combination of size- and shape-dependent physical properties along with their simple fabrication and processing techniques make MoS_2 nanomaterials, a promising candidate for a wide range of applications. The properties of the individual particles and their mutual interactions determine important features of nanomaterial systems. For example, optical properties are highly dependent on the size, shape, and crystallinity of the MoS_2 nanomaterials. However, controlled synthesis with a narrow size distribution and uniform shape remains an important issue in photocatalytic applications.

2.2. Synthesis of MoS_2 thin films

Chemical vapor deposition (CVD) is one of the most popular methods for fabricating thin films of few-layered MoS_2 nanosheets [10, 11]. In addition, impurity-assisted methods are

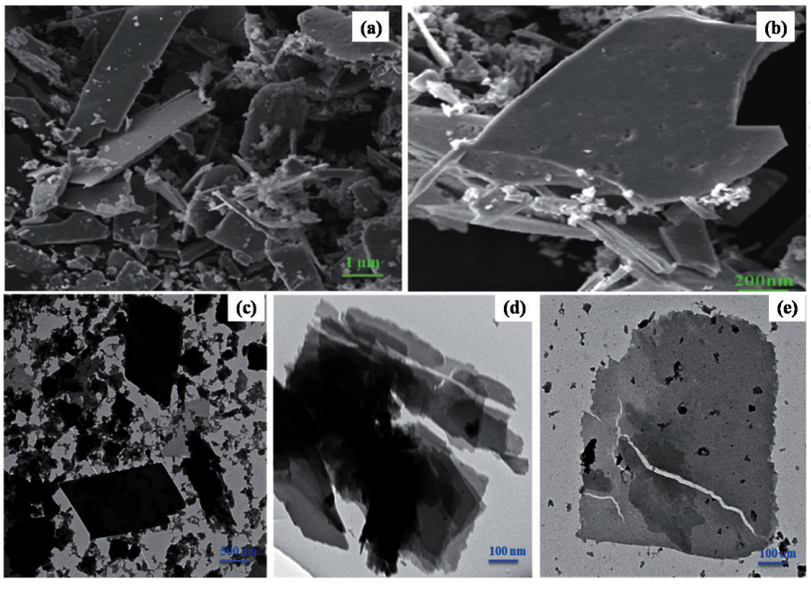

Figure 1. SEM (a,b) and TEM (c-e) images of solvothermally- synthesized MoS_2 nanosheets [6].

presently gaining much attention for increasing the grain size and decreasing the growth temperature. The growth conditions of single-layer MoS_2 in a CVD system depend on the nature of the substrate and the surface treatments used. Kinetic effects and on-off stoichiometric growth conditions can be used to produce different shapes in MoS_2 nanosheets, including star and dendrite shapes. The controllability and reproducibility of shape control are still being improved. In photocatalyst applications, the crystallinity and morphology strongly affect the device performance. Heterostructured MoS_2-based layered composite structures have recently been a focus in fundamental semiconductor technology.

The simplest way to develop a monolayer MoS_2 analog to graphene is the Scotch-tape exfoliation method from bulk MoS_2 along the direction of van der Waals interaction. Repeated exfoliation of bulk MoS_2 decreases the number of MoS_2 layers, eventually producing few- to single-layer MoS_2. However, this method is difficult for large-scale production due to the poor size controllability. To synthesize MoS_2 thin films on a large scale, three important techniques are mostly applied by researchers: thermal vapor sulfurization (TVS), dip coating, and CVD. CVD is the most prominent technique and is used with gasified Mo- and S-containing species that react and deposit on the surface of a substrate. The major difference between the CVD and TVS approaches is the state of Mo source: a solid Mo source is used in TVS, whereas a gasified Mo source is used in a CVD system. CVD systems can be classified according to energy source as (i) hot-walled thermal CVD, (ii) plasma CVD, and (iii) metal organic CVD, among others.

Hot-walled thermal CVD systems are widely used to synthesize MoS_2 nanosheets. Both sources of Mo and sulfur are gasified and transported to the surface of a substrate, adsorbed, and decomposed into reactive atoms, which results in the formation of covalent bonds and the growth of MoS_2 nanosheets. Byproducts and unreacted species are removed by the carrier gas. MoO_3, $Mo(CO)_6$, and $MoCl_5$ are widely used as Mo sources, while elemental sulfur and H_2S are used as sulfur sources, and N_2 or Ar is used as a carrier gas. $Mo(CO)_6$ has recently attracted attention and was successfully applied for large-scale production of MoS_2 thin film.

CVD systems can also be classified according to the design and features into four categories: (i) single-zone, (ii) two-zone, (iii) three-zone, and (iv) two-flow CVD systems. Two-flow CVD systems are the most sophisticated and are designed with three-zone CVD systems and a one-zone CVD system. The main features of a two flow-system are (i) independent control of the temperatures of the Mo and sulfur sources and the flow rates of each carrier gas for both sources, and (ii) the Mo source can be completely adjusted or stopped during when ramping and lowering the temperatures. Therefore, the growth rate of thin film can be controlled easily with a two-flow CVD system compared to conventional ones. However, careful attention is needed to obtain high-quality MoS_2 nanosheets.

Generally, the growth rate depends on various parameters, including the nature of the source materials, the temperature ranges of the sources and substrates, the system pressure, the vacuum levels, the type of substrates, and the type of carrier gas. However, unified conditions for the synthesis of MoS_2 nanosheets have not been developed due to the lack of a common practice and a unique CVD system design. The temperature ranges of the Mo and sulfur sources are 500–800°C and 130–300°C, respectively. The reaction temperature range of CVD systems is 650–1000°C, and the range of low rate of the carrier gas is 1–800 sccm. The duration ranges

http://dx.doi.org/10.5772/67825

from 30 s to 60 min. Some researchers synthesize MoS_2 nanosheets under reduced pressure or at atmospheric pressure.

Generally, the different shapes of synthesized MoS_2 nanosheets reflect the crystal structure. Hexagonal nanosheets consist of S-zig-zag and Mo-zig-zag termination sides and form triangle shapes that can be grown under different Mo and S source ratios. If either a small excess of the Mo or sulfur source is used, the shape becomes a truncated triangle instead of a perfect triangle. Initially, the MoS_2 nanosheets grow as a hexagonal shape, which changes to a triangle over time. When the Mo and sulfur sources reach a critical point, the MoS_2 nanosheets become star-shaped. For instance, a large excess amount of the sulfur source can facilitate the growth of only Mo-zig-zag termination sides in hexagonal MoS_2 nanosheets with suppression of S-zig-zag termination side growth, which results in the formation of a star shape.

Dendritic MoS_2 nanosheets form in the case of large flow rates of Mo and sulfur sources. These large flow rates create a thinner boundary layer, which results in the formation of dendritic shapes. Nonoptimal growth conditions cause round-shaped MoS_2 nanosheets with poor crystallinity. Surface treatment of a suitable substrate is very important for obtaining highly crystalline MoS_2 nanosheets. A hydrophilic substrate can be used to obtain few-layer MoS_2 nanosheets, whereas monolayer MoS_2 nanosheets can be obtained by using a superhydrophobic substrate. However, the exact mechanism of forming a monolayer on a superhydrophobic substrate is still not clear.

Park et al. [12] fabricated a thin film transistor (TFT) based on CVD-grown single-layer MoS_2, and the photoresponsive current and voltage characteristics of the TFT were measured with varying intensities of incident light. The photocurrent and mobility increased with increasing light intensity due to the contribution of photoinduced charge carriers from the valance band and trap states of the single-layered MoS_2. An exfoliated single-layer MoS_2-based TFT by Lin et al. exhibited higher mobility than the one based on CVD-grown MoS_2 [13]. However, the main advantage of CVD is the relatively large area of samples with homogenous qualities [14]. The CVD method has been used to grow MoS_2 directly on different dielectric substrates [15]. MoS_2 with photocatalytic properties have become an interesting candidate for the photodegradation of organic dye, hydrogen evolution, and CO_2 reduction, with the advantages of chemical and photostability.

3. Photocatalytic properties of MoS_2

The photocatalysis process involves the conversion of solar energy into chemical energy. The main goal for researchers is maximum utilization of the solar energy to enable the practical use of photocatalysts. However, photocatalytic ability has still been limited due to the fast recombination effect of electron-hole pairs and an insufficient absorption coefficient. Therefore, enhancing the efficiency of photocatalysts under visible light still remains a challenge for practical applications.

Many semiconductor oxides, sulfides, and nitrides have been used as photocatalysts for various applications. However, most sulfides and nitrides have lower band gaps, which limit usage due to stability issues of these materials in an aqueous medium. This issue is an important

one to solve to promote the use of these materials. The band gap of the oxides is higher than that of sulfides, and the absorption edge is only in the UV region. This limits the usage in the solar spectrum, although the material has good stability in an aqueous medium. The main characteristics of an ideal photocatalyst are maximum absorption in the visible solar spectrum, favorable band edges for promoting reactions, environmental friendliness, low cost, good stability, and reusability [16].

The band gap value of MoS_2 (1.9 eV) photoelectrodes and their considerably lower valence band edge than the water oxidation potential are favorable for water splitting through photo-electro-chemical techniques. The theoretical photocurrent density of chemically exfoliated MoS_2 is ~17.6 mA/cm^2 at 0.0 V vs. RHE under solar irradiation [17], and the solar energy conversion efficiency is ~18.7% for an ideal PEC cell. However, the photocatalytic activity of MoS_2 is limited by the factors mentioned thus far, which lead to low efficiencies and require larger potential to promote the photo-assisted water oxidation process [18]. Many researchers have tried to overcome these drawbacks of MoS_2 by decreasing the recombination rate through forming a composite or heterogeneous structure, as well as enhancing the conductivity by doping with metal and promoting the charge carrier transferability [19–22].

Apart from water-splitting applications, the photocatalytic performance of MoS_2 can be used for the degradation of organic compounds in waste water treatment applications. Vattikuti et al. [23] reported the mechanism of the degradation of rhodamine B (RhB) dye. The photosensitization of the RhB dye first takes place when charge transfer occurs from the valence band of the dye to the conduction band of the photocatalyst. This is followed by the initial photocatalytic reaction, where MoS_2 generates electron-hole pairs under photoirradiation. The electrons transfer from the valence band of MoS_2 to the conduction band and settle down holes within the valence band. The photoinduced electrons of MoS_2 produce intermediate superoxide radicals (O_2^-) by responding with chemisorbed oxygen on the photocatalyst surface and oxygen in the aqueous solution. The O_2^- radicals react with dissociated water (H^+) to form $\cdot HO_2$ and H_2O_2. In addition, hydroxyl groups (OH^-) are formed on the catalyst surface by the reaction with photoinduced holes (h^+) by absorbed water (OH_2). Thus, these generated radicals along with intermediate species react with RhB dye and degrade it into nontoxic organic compounds as follows:

$$RhB + h\upsilon \rightarrow RhB^{\cdot} \quad (1)$$

$$RhB^{\cdot} + MoS_2 \rightarrow RhB^{\cdot} + MoS_2\,(e_{CB}^-) \quad (2)$$

$$MoS_2 + h\upsilon \rightarrow MoS_2\,(e_{CB}^- + h_{VB}^+) \quad (3)$$

$$H_2O \rightarrow H^+ + OH^- \quad (4)$$

$$e_{CB}^- + O_2 \rightarrow O_2^{\bullet -} \quad (5)$$

$$O_2^{\bullet -} + H^+_{aq} \rightarrow HO_2^{\cdot} \quad (6)$$

$$HO_2^{\cdot} + HO_2^{\cdot} \leftrightarrow H_2O_2 + O_2 \quad (7)$$

$$h_{VB}^+ + OH^-_{aq} \rightarrow OH^{\cdot -} \quad (8)$$

$$RhB^{\cdot}/RhB^{\cdot +} + (O_2^{\bullet -}, HO_2^{\cdot}, H_2O_2, OH^{\cdot -}) \rightarrow \text{Degradation products}\ldots. \quad (9)$$

http://dx.doi.org/10.5772/67825

MoS_2 is also a good photocatalyst for photocatalytic oxidative desulfurization [24]. Sulfur compounds in fuel convert into SOx, which causes air pollution and acid rain. Generally, the hydrodesulfurization (HDS) process is widely employed commercially to remove sulfur species at high temperature (350°C) and pressure (7 MPa). Recently, photooxidative desulfurization has been popular because it is economical and has high efficiency [25, 26], which can provide cleaner and more efficient removal of sulfur species from petroleum fuel oils [27]. Lia et al. reported that CeO_2/MoS_2 and attapulgite showed excellent electron transfer within the composite and favor the desulfurization process under solar irradiation [24]. MoS_2-assisted nanocomposite systems have led to a new era in research and show promise as a high-activity and low-cost photocatalyst for applications such as deep desulfurization. Thurston et al. [28] and Wilcoxon et al. [29] reported on MoS_2 nanoparticles with diameters at 3–4.5 nm as a catalyst for the degradation of phenol, 4-chlorophenol, and pentachlorophenol under visible light irradiation.

4. Literature reviews on MoS_2 photocatalytic mechanism

We emphasize three different forms of MoS_2 that have been studied. Ongoing research on MoS_2 nanoparticles as a photocatalyst is addressed first, followed by studies associated with MoS_2 composites. This section concludes with a discussion on thin-coated MoS_2.

4.1. Unary MoS_2 photocatalyst

A high aspect ratio plays a key role in the photocatalytic activity of materials, and researchers have concentrated on reducing the size of the photocatalyst and improving the photocatalytic activities of these materials by making nanoscale MoS_2. Many approaches have been used to synthesize nanocrystalline MoS_2 with different morphologies, including ultrasonic cracking [30], hydrothermal methods [31–33], chemical synthesis [34], combustion methods [35–38], wet chemical methods, and coprecipitation methods [23, 38–40].

Vattikuti et al. synthesized MoS_2 multiwall nanotubes (MWNTs) by a wet chemical method assisted by H_2O_2 solvent as a growth promotor [41]. The photocatalytic performance of MoS_2 MWNTs was applied to the degradation of RhB. The MoS_2 MWNTs exhibited excellent photocatalytic performance compared to pure MoS_2. The higher photocatalytic activity of MoS_2 MWNTs was ascribed to the large number of active sites with a high specific surface area. The performance of the optimal amount of 0.5 wt% MoS_2 MWNTs was attributed to the higher transfer of electrons and holes during the photoreaction, which effectively suppressed the recombination of the electron-hole pairs and enhanced the degradation efficiency.

Zhou et al. [42] hydrothermally synthesized porous MoS_2 without any sacrificial template using sodium molybdate and thioacetamide as Mo and S sources. Porous MoS_2 showed 89.2% degradation efficiency of MB under 150 min of visible light irradiation. MB photodegradation in the presence of porous MoS_2 was obtained with a pseudo-first-order kinetic reaction rate of 0.01484 min^{-1}. Polycrystalline porous MoS_2 shows attractive photocatalytic activities that

are ascribed to the active edge sites. Sheng et al. [43] synthesized flower-like MoS_2 spheres via the hydrothermal method and studied the effects of excess sulfur source on the flower-like MoS_2 structure. To obtain the flower-like MoS_2 spheres, MoO_3, and potassium thiocyanate (KSCN) were used as Mo and S sources with different S/Mo ratios. The optimal S/Mo ratio of 2.75 resulted in the highest degradation rate of MB with a degradation rate of 0.03833 min^{-1} under 90 min of visible light irradiation. The increased photocatalytic performance was ascribed to the increased exposed area of the [43] facets with the optimal S/Mo ratio in the hydrothermal synthesis environment. The sheet thickness of the MoS_2 spheres increased with the S/Mo ratio and enhanced the photocatalytic activity.

Liu et al. [44] produced MoS_2 nanosheets by a hydrothermal method with H_2SiO_3 (silicic acid) hydrogel containing ammonium molybdate hydrate and thiourea precursors. MoS_2 nanosheets were obtained by removing the H_2SiO_3. These MoS_2 nanosheets have a high specific surface area (S_{BET}) of 37.8 m^2g^{-1} and present notable absorption of MO under visible light rather than ultraviolet light in 70 min of irradiation. Different shapes of MoS_2 nanosheets were obtained by varying the concentration of silicic acid with MoS_2 molar ratios of 2.5 and 0.8, such as leaf-shaped and flower-shaped MoS_2 nanosheets. These provide steric hindrance for MoS_2 nanosheet growth. The amount of hydroxyl radicals was highest at pH 2 and decreased when increasing to pH 9. The OH group plays a major role in MO photodegradation in the catalytic system. The reaction time, initial concentration, catalyst dosage, and local structures are also key factors that affect the photocatalytic performance of the materials.

4.2. Binary MoS_2 photocatalysts

This section reviews the effect of heterogeneous structures or composite forms of MoS_2 on the photocatalytic properties. Combining MoS_2 with metals or nonmetals and semiconductor materials is a common practice for enhancing photocatalytic performance by facilitating and promoting efficient charge transfer at the interfaces. Similar attempts have been made for other classes of materials to improve photocatalytic activity, including Fe_2O_3, TiO_2, and ZnO.

Thurston et al. [28] demonstrated that MoS_2 nanoparticles with diameter of 8–10 nm could not photodegrade phenol under visible light due to poor light absorption. Hence, they sensitized TiO_2 nanoparticles with MoS_2 nanoparticles, which enabled photodegradation under visible light irradiation. This composite structure showed a blue shift in absorbance due to quantum confinement of the charge carriers [28, 45]. We recently reported improved photocatalytic performance of MoS_2 nanosheets decorated with mesoporous SnO_2 nanospheres by a facile two-step method [46]. We also observed the photocatalytic effect in the degradation of RhB with less than 50 min of UV light irradiation. The supported mesoporous SnO_2 nanoparticles significantly suppressed the recombination of electron-hole pairs compared to pure MoS_2 photocatalyst material. The improved photocatalytic performance of the MoS_2/SnO_2 composite was explained by two mechanisms: (i) the absorption ability of the MoS_2 nanosheets with active edges and (ii) enhanced electron transfer from SnO_2 to the MoS_2 nanosheets. This heterostructured composite facilitated effective electron transfer

from the CB of SnO_2 to the MoS_2 nanosheets and suppressed the recombination effect. Therefore, the SnO_2-decorated MoS_2 nanocomposite showed better photocatalytic performance than pure MoS_2. Photocorrosion is the main reason for the lower photocatalytic activity of the pure MoS_2.

Pourabbas et al. [47] synthesized a hybrid MoS_2/TiO_2 composite using a modified hydrothermal method. The changes from the normal hydrothermal method included using sodium lauryl sulfate as a surface-active agent with 1-octanol as a cosurfactant and varying reaction temperature. The hybrid composite was used as a photocatalyst for the photo-oxidative removal of phenol. The composite showed enhanced photocatalytic performance in the phenol degradation under both UV (70 min) and visible light (24 min) compared to pure TiO_2 and MoS_2. The complete mineralization of phenol during the photo-oxidation reaction in 145 min of UV irradiation was indicated by HPLC chromatograms. Zhou et al. [48] and Bai et al. [49] did similar work and evaluated the photocatalytic performance of the MoS_2/TiO_2 composite for photodegradation of MB under visible light irradiation.

MoS_2-coated TiO_2 nanobelt composites showed excellent photocatalyst properties for RhB degradation under 33 min of visible light irradiation. The matched energies of the TiO_2@ MoS_2 composite are favorable for the charge transfer and suppress the recombination of electron-hole pairs. The photocatalytic hydrogen production was also enhanced. Liu et al. [50] synthesized a composite of TiO_2 nanobelts decorated with MoS_2 nanoparticles using a two-step hydrothermal method. The photocatalytic degradation of the TiO_2/MoS_2 composite was evaluated with RhB under 90 min of visible light irradiation. The sample with 40 wt% MoS_2 nanoparticles decorated on TiO_2 nanobelts showed the best photocatalytic performance, which was attributed to the prevented recombination of photoinduced electron-hole pairs. This sample showed a high photocatalytic reaction rate constant that is about 4.78 times that of pure TiO_2.

Cao et al. [51] synthesized MoS_2/TiO_2 hybrid composites by a two-step hydrothermal route. The MoS_2/TiO_2 hybrid composite showed excellent photocatalytic performance in the degradation of RhB in 100 min of visible-light irradiation in comparison to pure forms. The improvement in photocatalytic activity of the composite was mainly ascribed to the properly matching CB and VB energy levels and the enhanced separation efficiency of photoinduced electron-hole pairs at interfacial contacts of the composite. Wang et al. [52, 53] reported the *in situ* deposition of Ag_3PO_4 on graphene-like MoS_2 nanosheets via a wet chemical route. The goal was to improve the photocatalytic performance for the degradation of RhB in 20 min of visible light irradiation (>400 nm). The improved photocatalytic performance of the heterostructure of Ag_3PO_4/MoS_2 composite is ascribed to the efficient separation of photoinduced electron-hole pairs within the photocatalyst.

Ding et al. [54] synthesized a MoS_2-GO hydrogel composite using a hydrothermal method for MB degradation under 60 min of solar light irradiation. This composite showed enhanced photocatalytic performance in the degradation of MB with a maximum degradation rate of 99% for 60 min under solar light irradiation. The improvement was attributed to the increased light absorption and suppressed recombination effect of semiconductor photocatalysis.

Zhang et al. [55] synthesized MoS_2/rGO photocatalyst for the fluorescence detection of glutathione in a ·OH radical elimination system based on the reducing ability of glutathione under visible light irradiation. The MoS_2/rGO composite efficiently generated ·OH radicals and reduced ·OH radicals by the absorption of glutathione under visible light, which is reflected by a reduction of the fluorescence intensity due to the elimination of ·OH radicals. This kind of photocatalyst can be effectively implemented for the identification of glutathione in commercial drugs and human serum.

Wang et al. [56] synthesized $MoS_2/Bi_2O_2CO_3$ composites for RhB photodegradation under 150 min of visible light irradiation by a simple hydrothermal method. The effect of photocatalyst concentration on the photocatalytic efficiency was observed. This composite has more active sites of MoS_2 on $Bi_2O_2CO_3$, which promoted the photocatalytic performance by absorbing and decomposing more RhB pollutant than pure $Bi_2O_2CO_3$. The remarkable enhancement in the photocatalytic activity could be ascribed to the synergistic effect between the MoS_2 and $Bi_2O_2CO_3$ in the heterostructured composite. Li et al. [57] reported $MoS_2/BiVo_4$ hetero-nanoflower composites as an excellent photocatalyst for MB degradation with less than 120 min of sunlight irradiation.

Li et al. [58] successfully synthesized a 2D heterojunction photocatalyst of g-C_3N_4 coupled with MoS_2 nanosheets using a simple impregnation and calcination method. The g-C_3N_4/MoS_2 composite promoted the charge transfer and improved the separation efficiency of photo-induced electron–hole pairs in RhB and MO degradation under 180 min of visible light irradiation. Jo et al. [59] synthesized MoS_2 nanosheets loaded with ZnO-gC_3N_4 ternary photocatalyst for MB photodegradation under 60 min of UV-visible light irradiation. The ternary nanocomposite significantly improved the lifetime of charge carriers and facilitated effective migration and charge separation at the interface.

Zhang et al. [60] synthesized a ternary composite system of TiO_2/MoS_2@zeolite using a facile ultrasonic-hydrothermal synthesis method with $TiCl_4$ as a Ti source and zeolite as a carrier. The photocatalytic performance was investigated for MO degradation for 60 min under xenon long-arc lamps as a visible light source. The photoinduced electrons and holes are collected in the CB of MoS_2 and the VB of TiO_2. The more negative bottom CB energy of MoS_2 and more positive top CB energy of TiO_2 allow the photoinduced electrons in the CB of MoS_2 to reduce the absorbed O_2 into $\cdot O_2^-$. ·OH can be produced easily in the VB of TiO_2, and the $\cdot O_2^-$ and ·OH active species lead to MO degradation. **Figure 2** shows the possible photocatalytic mechanism of both unary and binary photocatalysts.

Hu et al. [62] synthesized MoS_2/Kaolin composites by calcining a MoS_3/kaolin precursor in H_2 under strong acidic conditions. The composite had a specific surface area of 16 m^2g^{-1} and showed a positive photocatalytic effect on MO degradation under 105 min of visible light irradiation. This performance was attributed to the good absorption capacity in the visible light region. The photocatalyst has remarkable stability and can be regenerated and reused via filtration. The deactivating photocatalyst could be reactivated even after photocatalytic reaction at 450°C for 30 min under H_2. The photocatalytic performance of exfoliated MoS_2 was also investigated, and the relationship between the morphology of nano-MoS_2 and the photocatalytic properties was discussed [63]. The photocatalytic performance of this and

http://dx.doi.org/10.5772/67825

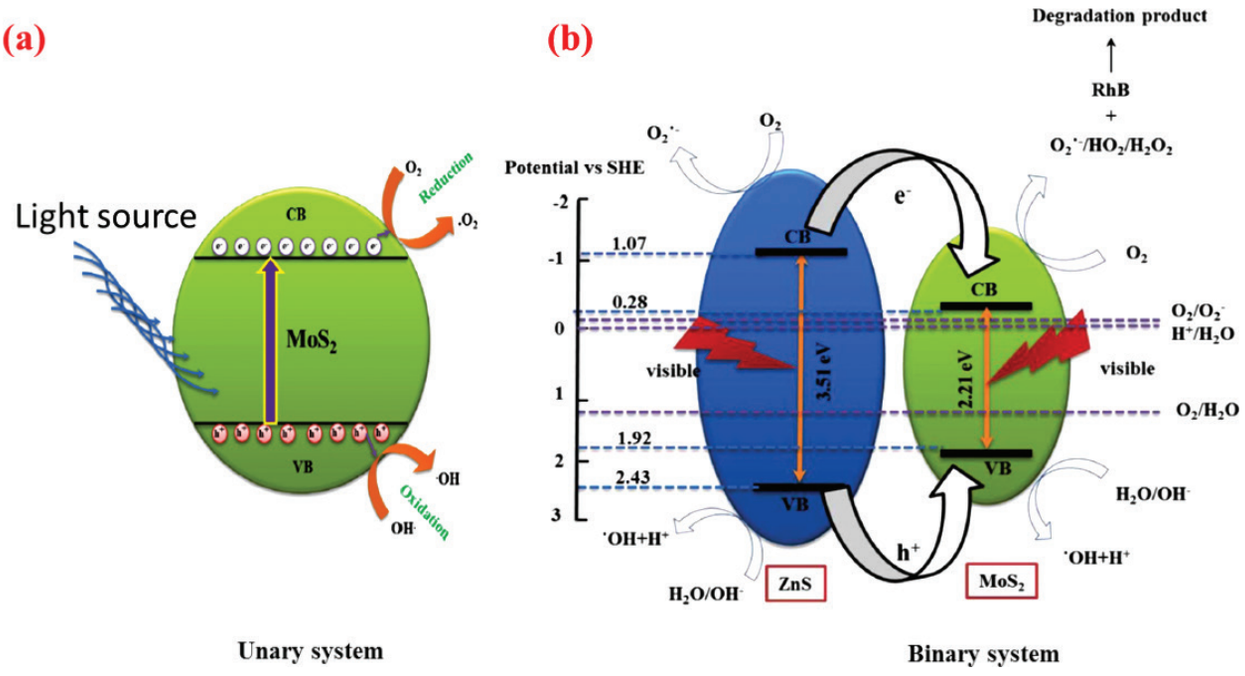

Figure 2. Schematic diagram of photocatalytic mechanism of (a) unary [8] and (b) binary photocatalyst [61].

other heterostructured composites are influenced by the quantity of photocatalyst, initial concentration of pollutant or dye, pH, irradiation time, type of light source, and degradation temperature.

5. Summary

Layered MoS_2 materials have attracted continuously increasing interest and demand, and preparation techniques have been successfully developed. We have a provided a detailed overview of the photocatalytic performance of MoS_2 nanomaterials, three different types of MoS_2 photocatalyst systems were distinguished according to their structural components(single component, heterostructured, and doped MoS_2). There is great interest in preparing various MoS_2 photocatalyst systems by novel strategies, as well as hierarchical MoS_2 structures with special functionalities. Therefore, there is ongoing effort to develop new MoS_2 materials with novel structures and their applications.

The importance of MoS_2 photocatalysts has been highlighted for the degradation of pollutant from contaminated waste water through solar light irradiation. There have been a number of advances in this field, including the development of materials with lower band gap, low cost, and increased stability and reusability. These developments make MoS_2 photocatalyst a promising candidate for further practical advances in the future. However, degradation rates are still generally low, the materials are somewhat unstable over repeated usage, and there is great variability in the reported reduction rate and efficiencies of these systems. It is of great importance that reduction rates be reproduced from

one lab to another, and repeatability and reusability are currently some of the significant deficiencies in the field. In future, scientists should focus on material design and the realization of practical applications.

Acknowledgements

This work was conducted under the framework of the National Research Foundation of Korea (NRF) and funded by the Ministry of Science, ICT, and Future Planning (2014 R1A2A2A01007081).

Author details

Surya Veerendra Prabhakar Vattikuti[1]* and Chan Byon[2]

*Address all correspondence to: vsvprabu@gmail.com

1 School of Mechanical Engineering, Yeungnam University, Gyeongsan-si, Gyeongsangbuk-do, Republic of Korea

2 School of Mechanical and Nuclear Engineering, Ulsan National Institute of Science and Technology, Ulsan, Republic of Korea

References

[1] Tenne R, Margulis L, Genut M, Hodes G. Polyhedral and cylindrical structures of tungsten disulphide. Nature. 1992;**360** (6403):444–446.

[2] Youngblood WJ, Lee SA, Maeda K, Mallouk ThE. Visible light water splitting using dyesensitized oxide semiconductors. Accounts of Chemical Research. 2009;**42**(12): 1966–1973.

[3] Rao CNR, Nath M. Inorganic nanotubes. Dalton Transactions. 2003;**1**:1.

[4] Splendiani A, Sun L, Zhang Y, Li T, Kim J, Chim CY, Galli G, Wang F. Emerging photoluminescence in monolayer MoS_2. Nano Letters. 2010;**10**(4):1271.

[5] Visic B, Dominko R, Klanjsek Gunde R, Hauptman N, Skapin SD, Remskar M. Optical properties of exfoliated MoS_2 coaxial nanotubes – Analogues of graphene. Nanoscale Research Letters. 2011;**6**:593.

[6] Prabhakar Vattikuti SV, Byon C, Venkata Reddy C, Venkatesh B, Shim J. Synthesis and structural characterization of MoS_2 nanospheres and nanosheets using solvothermal method. Journal of Materials Science. 2015;**50**:5024–5038.

[7] Prabhakar Vattikuti SV, Byon C. Synthesis and characterization of molybdenum disulfide nanoflowers and nanosheets: Nanotribology. Journal of Nanomaterials. 2015;**2015**, Article ID 710462:1–11.

[8] Prabhakar Vattikuti SV, Byon C, Venkata Reddy Ch. Synthesis of MoS_2 multi-wall nanotubes using wet chemical method with H_2O_2 as growth promoter. Superlattices and Microstructures. 2015;**85**:124–132.

[9] Lukowski MA, Daniel AS, Meng F, Forticaux A, Li L, Jin S. Enhanced hydrogen evolution catalysis from chemically exfoliated metallic MoS_2 nanosheets. Journal of American Chemical Society. 2013;**135**(28):10274–10277.

[10] Han SA, Bhatia R, Kim SW. Synthesis, properties and potential applications of two-dimensional transition metal dichalcogenides. Nano Convergence. 2015;**2**:17.

[11] Li X, Zhu H. Two-dimensional MoS_2: Properties, preparation, and applications. Journal of Materiomics. March 2015;**1**(1):33–44.

[12] Park HJ, Kim MS, Kim J, Joo J. Photo-responsive transistors of CVD grown single-layer MoS_2 and its nanoscale optical characteristics. Current Applied Physics. 2016;**16**:1320–1325.

[13] Lin MW, Kravchenko II, Fowlkes J, Li X, Puretzky AA, Rouleau CM, Geohegan DB, Xiao K. Thickness-dependent charge transport in few-layer MoS2 field-effect transistors. Nanotechnology. 2016;**27**:165203.

[14] Yin Z, Li H, Li H, Jiang L, Shi Y, Sun Y, Lu G, Zhang Q, Chen X, Zhang H. Single-Layer MoS2 Phototransistors. ACS Nano. 2012;**6**:74.

[15] Chen J, Guo Y, Jiang L, Xu Z, Huang L, Xue Y, Geng D, Wu B, Hu W, Yu G, Liu Y. Chemical Vapor Deposition of High-Quality Large-Sized MoS2 Crystals on Silicon Dioxide Substrates. Advanced Materials. 2014;**26**:1348.

[16] Liu G, Niu P, Yin LC, Cheng HM. α-Sulfur crystals as a visible-light-active photocatalyst. Journal of American Chemical Society. 2012;**134**:9070–9073.

[17] Chen Sh, Thind SS, Chen A. Nanostructured materials for water splitting – State of the art and future needs: A mini-review. Electrochemistry Communications. 2016;**63**:10–17.

[18] Yu H, Zhou W, Li G, Jin R. Some strategies in designing highly efficient photocatalysts for degradation of organic pollutants in water. ACS Symposium Series. 2014;**1186**:139–160 ISBN13: 9780841230187eISBN: 9780841230194.

[19] Barber J, Tran PD. From natural to artificial photosynthesis. 2013. Jornal of the royal society interface, 2013; **10**:20120984.

[20] Gao M, Liang J, Zheng Y, Xu Y, Jiang J, Gao Q, Li J, Yu SH. An efficient molybdenum disulfide/cobalt diselenide hybrid catalyst for electrochemical hydrogen generation. Nature Communications. 2015;**6**:5982–5987.

[21] Mohamed RM, McKinney DL, Sigmund WM. Enhanced nanocatalysts. Materials Science and Engineering R 2012;**73**:1–13.

[22] Bai S, Jiang W, Li Zh, Xiong Y. Surface and interface engineering in photocatalysis. ChemNanoMat. 2015;**1**:223–239.

[23] Vattikuti SVP, Byon Ch, Reddy ChV. Synthesis of MoS_2 multi-wall nanotubes using wet chemical method with H_2O_2 as growth promoter. Superlattices and Microstructures. 2015;**85**:124–132.

[24] Lia X, Zhang Z, Yao Ch, Lu X, Zhao XX, Ni Ch. Attapulgite-CeO_2/MoS_2 ternary nanocomposite for photocatalytic oxidative desulfurization. Applied Surface Science. 2016;**364**:589–596.

[25] Yang D, Yang S, Jiang ZY, Yu SN, Zhang JL, Pan FS, Cao XZ, Wang BY, Yang J. Polydimethyl siloxane–graphene nanosheets hybrid membranes with enhanced pervaporative desulfurization performance. Journal of Membrane Science. 2015;**487**:152–161.

[26] Wang R, Wan JB, Li YH, Sun HW. An improvement of MCM-41 supported phosphoric acid catalyst for alkylation desulfurization of fluid catalytic cracking gasoline. Fuel. 2015;**143**:504–511.

[27] Zhu WS, Xu YH, Li HM, Dai BL, Xu H, Wang C, Chao YH, Liu H. Photocatalytic oxidative desulfurization of dibenzothiophene catalyzed by amorphous TiO_2 in ionic liquid. Korean Journal of Chemical Engineering. 2014;**31**:211–217.

[28] Thurston TR, Wilcoxon JP. Photooxidation of organic chemicals catalyzed by nanoscale MoS_2. The Journal of Physical Chemistry B. 1999;**103**:11–17.

[29] Wilcoxon JP. Catalytic photooxidation of pentachlorophenol using semiconductor nanoclusters. The Journal of Physical Chemistry B. 2000;**104**:7334–7343.

[30] Zheng X, Zhu L, Yan A, Bai Ch, Xie Y. Ultrasound-assisted cracking process to prepare MoS_2 nanorods. Ultrasonics Sonochemistry. 2004;**11**:83–88.

[31] Pu FL, Chi Ch, Zakari S, Liew T, Yarmo MA, Huang NM. Preparation of transition metal sulide nanoparticles via hydrothermal route. Sains Malaysiana. 2010;**39**(2):243–248.

[32] Lin H, Chen X, Li H, Yang M, Qi Y. Hydrothermal synthesis and characterization of MoS_2 nanorods. Materials Letters. 2010;**64**:1748–1750.

[33] Chen X, Li H, Wang Sh, Yang M, Qi Y. Biomolecule-assisted hydrothermal synthesis of molybdenum disulfide microspheres with nanorods. Materials Letters. 2012;**66**:22–24.

[34] Tian Y, Zhao J, Fu W, Liu Y, Zhu Y, Wang Z. A facile route to synthesis of MoS_2 nanorods. Materials Letters. 2005;**59**:3452–3455.

[35] Mukasyan AS, Manukyan Kh. Combustion/micropyretic synthesis of atomically thin two-dimensional materials for energy applications. Current Opinion in Chemical Engineering. 2015;**7**:16–22.

[36] Rao CNR, Thomas PJ, Kulkarni GU. Nanocrystals: Synthesis, Properties and Applications. 2007. 95, Springer Berlin Heidelberg. ISBN 978-3-540-68752-8.

[37] Gonzalez-Cortes SL, Xiao T, Rodulfo-Baechler SMA, Green MLH. Impact of the urea–matrix combustion method on the HDS performance of Ni-MoS_2/-Al_2O_3 catalysts. Journal of Molecular Catalysis A: Chemical. 2005;**240**:214–225.

[38] Gonzalez-Cortes SL, Xiao T, Lin T, Green MLH. Influence of double promotion on HDS catalysts prepared by urea-matrix combustion synthesis. Applied Catalysis A: General. 2006;**302**:264–273.

[39] Hu KH, Wang YR, Hu XG, Wo HZ. Preparation and characterization of ball-like MoS_2 nanoparticles. Materials Science and Technology. 2007;**23**:242–246.

[40] Yu H, Liu Y, Brock SL. Synthesis of discrete and dispersible MoS_2 nanocrystals. Inorganic Chemistry. 2008;**47**:1428–1434.

[41] París JRS, Montes V, Boutonnet M, Järås S. Higher alcohol synthesis over nickel-modified alkali-doped molybdenum sulfide catalysts prepared by conventional coprecipitation and coprecipitation in microemulsions. Catalysis Today. 2015;**258**:294–303.

[42] Zhou Zh, Lin Y, Zhang P, Ashalley E, Shafa M, Li H, Wu J, Wang Zh. Hydrothermal fabrication of porous MoS_2 and its visible light photocatalytic properties. Materials Letters. 2014;**131**:122–124.

[43] Sheng B, Liu J, Li Z, Wang M, Zhu K, Qiu J, Wang J. Effects of excess sulfur source on the formation and photocatalytic properties of flower-likeMoS_2 spheres by hydrothermal synthesis. Materials Letters. 2015;**144**:153–156.

[44] Liu W, Hu Q, Mo F, Hu J, Feng Y, Tang H, Yea Sh, Miao H. Photo-catalytic degradation of methyl orange under visible light by MoS_2 nanosheets produced by H_2SiO_3 exfoliation. Journal of Molecular Catalysis A: Chemical. 2014;**395**:322–328.

[45] Wilcoxon JP, Samara GA. Strong quantum-size effects in a layered semiconductor: MoS_2 nanoclusters. Physical Review B. 1995;**51**:7299–7302.

[46] Vattikuti SVP, Byon Ch, Reddy ChV, Ravikumar RVSSN. Improved photocatalytic activity of MoS_2 nanosheets decorated with SnO_2 nanoparticles. RSC Advances. 2015;**5**:86675–86684.

[47] Pourabbas B, Jamshidi B. Preparation of MoS_2 nanoparticles by a modified hydrothermal method and the photo-catalytic activity of MoS_2/TiO_2 hybrids in photo-oxidation of phenol. Chemical Engineering Journal. 2008;**138**:55–62.

[48] Zhou H, Gu T, Yang D, Jiang Zh, Zeng J. Photocatalytic degradation of methylene blue on MoS_2/TiO_2 nanocomposite. Advanced Materials Research. 2011;**197–198**:996–999.

[49] Bai S, Wang L, Chen X, Du J, Xiong Y. Chemically exfoliated metallic MoS_2 nanosheets: A promising supporting co-catalyst for enhancing photocatalytic performance of TiO_2 nanocrystals. Nano Research. 2015;**8**(1):175–183.

[50] Liu H, Lv T, Zhu Ch, Su X, Zhu Zh. Efficient synthesis of MoS_2 nanoparticles modified TiO_2 nanobelts with enhanced visible-light-driven photocatalytic activity. Journal of Molecular Catalysis A: Chemical 2015;**396**:136–142.

[51] Cao L, Wang R, Wang D, Li X, Jia H. MoS_2-hybridized TiO_2 nanosheets with exposed {001} facets to enhance the visible-light photocatalytic activity. Materials Letters 2015;**160**:286–290.

[52] Wang P, Shi P, Hong Y, Zhou X, Yao W. Facile deposition of Ag_3PO_4 on graphene-like MoS_2 nanosheets for highly efficient photocatalysis. Materials Research Bulletin 2015;**62**:24–29.

[53] Wang L, Chai Y, Ren J, Ding J, Liu Q, Dai W. Ag_3PO_4 nanoparticles loaded on 3D flower-like spherical MoS_2: A highly efficient hierarchical heterojunction photocatalyst. Dalton Transactions 2015;**44**:14625–14634.

[54] Ding BY, Zhou Y, Nie W, Chen P. MoS_2–GO nanocomposites synthesized via a hydrothermal hydrogelmethod for solar light photocatalytic degradation of methylene blue. Applied Surface Science 2015;**357**:1606–1612.

[55] Zhang N, Ma W, Han DX, Wang L, Wu T, Niu L. The fluorescence detection of glutathione by · OH radicals' elimination with catalyst of MoS_2/rGO under full spectrum visible light irradiation. Talanta 2015;**144**:551–558.

[56] Wanga Q, Yun G, Bai Y, An N, Lian J, Huang H, Su B. Photodegradation of rhodamine B with $MoS_2/Bi_2O_2CO_3$ composites under UV light irradiation. Applied Surface Science 2014;**313**:537–544.

[57] Li H, Yu K, Lei X, Guo B, Fu H, Zhu Z. Hydrothermal synthesis of novel $MoS_2/BiVO_4$ hetero-nanoflowers with enhanced photocatalytic activity and a mechanism investigation. The Journal of Physical Chemistry C 2015;**119**:22681–22689.

[58] Li J, Liu E, Ma Y, Huc X, Wan J, Sun L, Fan J. Synthesis of MoS_2/g-C_3N_4 nanosheets as 2D heterojunction photocatalysts with enhanced visible light activity. Applied Surface Science 2016;**364**:694–702.

[59] Jo W, Lee YJ, Selvam NCS. Synthesis of MoS_2 nanosheets loaded ZnO-g-C_3N_4 nanocomposites for enhanced photocatalytic applications. Chemical Engineering Journal 2016;**289**:306–318.

[60] Zhang W, Xiao X, Zheng L, Wan C. Fabrication of TiO_2/MoS_2@zeolite photocatalyst and its photocatalytic activity for degradation of methyl orange under visible light. Applied Surface Science 2015;**358**:468–478.

[61] Vattikuti SVP, Byon Ch, Reddy ChV. ZrO_2/MoS_2 heterojunction photocatalysts for efficient photocatalytic degradation of methyl orange. Electronic Materials Letters. 2016;**12**(6):812–823.

[62] Hu KH, Liu Zh, Huang F, Hu XG, Han ChL. Synthesis and photocatalytic properties of nano-MoS_2/kaolin composite. Chemical Engineering Journal 2010;**162**:836–843.

[63] Hu KH, Hu XG. Formation, exfoliation and restacking of MoS_2 nanostructures. Materials Science and Technology 2009;**25**:407–414.